Modeling of Glow Discharge Sources with Flat and Pin Cathodes and Implications for Mass Spectrometric Analysis

Annemie Bogaerts and Renaat Gijbels
Department of Chemistry, University of Antwerp, Wilrijk-Antwerp, Belgium

A set of three-dimensional models for a direct current glow discharge in argon, developed previously in our group, is applied to analytical glow discharge cells with either flat or pin-type cathodes. Among other quantities, the densities of the plasma species are calculated and compared for these two cathode shapes. A comparison is also made for the computed argon and sputtered cathode (copper) ion currents leaving the glow discharge cell and entering the mass spectrometer, because this is of major interest from the analytical point of view. Finally, for the pin cell, the influence of sampling distance (i.e., distance between cathode pin and exit slit to the mass spectrometer) on the calculated plasma quantities is investigated. (J Am Soc Mass Spectrom 1997, 8, 1021–1029) © 1997 American Society for Mass Spectrometry

Glow discharges find applications in analytical chemistry as spectroscopic sources for mass spectrometry and optical spectrometric techniques [1]. Moreover, they are also extensively used for technological purposes [2]: for deposition of layers and plasma etching of surfaces, e.g., in the microelectronics industry, and also as plasma displays, as metal vapor ion lasers and as fluorescent lamps. To obtain good results in these application fields, a clear insight in the processes occurring in the glow discharge is desirable. We try to obtain this by mathematical modeling. In previous work, we have developed a set of three-dimensional models to describe the behavior of the different species present in a glow discharge used for analytical purposes [3–5]. Until now, the models were applied only to glow discharge cells with flat cathodes [3–7]. However, glow discharges with pin-type cathodes are also frequently used in analytical work [8–11]. Since our models have been developed in three dimensions, they can also be applied to glow discharge cells with pin-type cathodes, with only slight modifications.

In the case of cell geometries with flat cathodes, the modeling results were compared with experimental observations, to test the validity of the models. Three-dimensional density profiles of argon metastable atoms, and of sputtered atoms and ions, were measured by laser-induced fluorescence spectrometry, and reasonable agreement with the modeling results was reached [12, 13]. Also the current-voltage-pressure characteristics were more or less correctly predicted by the model, as was shown in refs 5 and 14. The calculated flux energy distributions of ions bombarding the cathode were also in good agreement with measurements performed with the VG9000 glow discharge mass spectrometer [15]. Finally, the experimentally found characteristic crater profiles, because of sputtering at the cathode could also satisfactorily be backed-up by our calculations [16]. Hence, from these comparisons with experiment, it could be concluded that the models present a realistic picture of the glow discharge. Therefore, it is expected that they will also be realistic for other geometries. In the present paper, the models will be applied to glow discharges both with pin and flat cathodes, and a comparison between these two geometries will be made.

Description of the Models

The models are explained in detail in refs 3–5, 12, 14, and 17–21 and only a brief overview will be given here. The species assumed to be present in the plasma include the argon gas atoms at rest uniformly distributed throughout the discharge, singly charged argon ions, fast argon atoms created from the argon ions, argon metastable atoms, electrons (fast and slow group), and sputtered analyte atoms and ions (copper is taken as an example). The behavior of these species is described with a combination of Monte Carlo and fluid models. Monte Carlo models are employed for the fast plasma species, which are not in equilibrium with the electric field [i.e., the fast electrons, and the argon ions, fast argon atoms and copper ions in the region close to the cathode (cathode dark space) where a strong electric field is present]. Fluid models are used for the slow plasma particles that can be considered to be in equilibrium with the electric field [i.e., the slow electrons,

Address reprint requests to Annemie Bogaerts, Department of Chemistry, University of Antwerp, Universiteitsplein 1, B-2610 Wilrijk-Antwerp, Belgium.

1044-0305/97/$17.00
PII S1044-0305(97)00120-7

Received February 12, 1997
Revised April 25, 1997
Accepted April 29, 1997

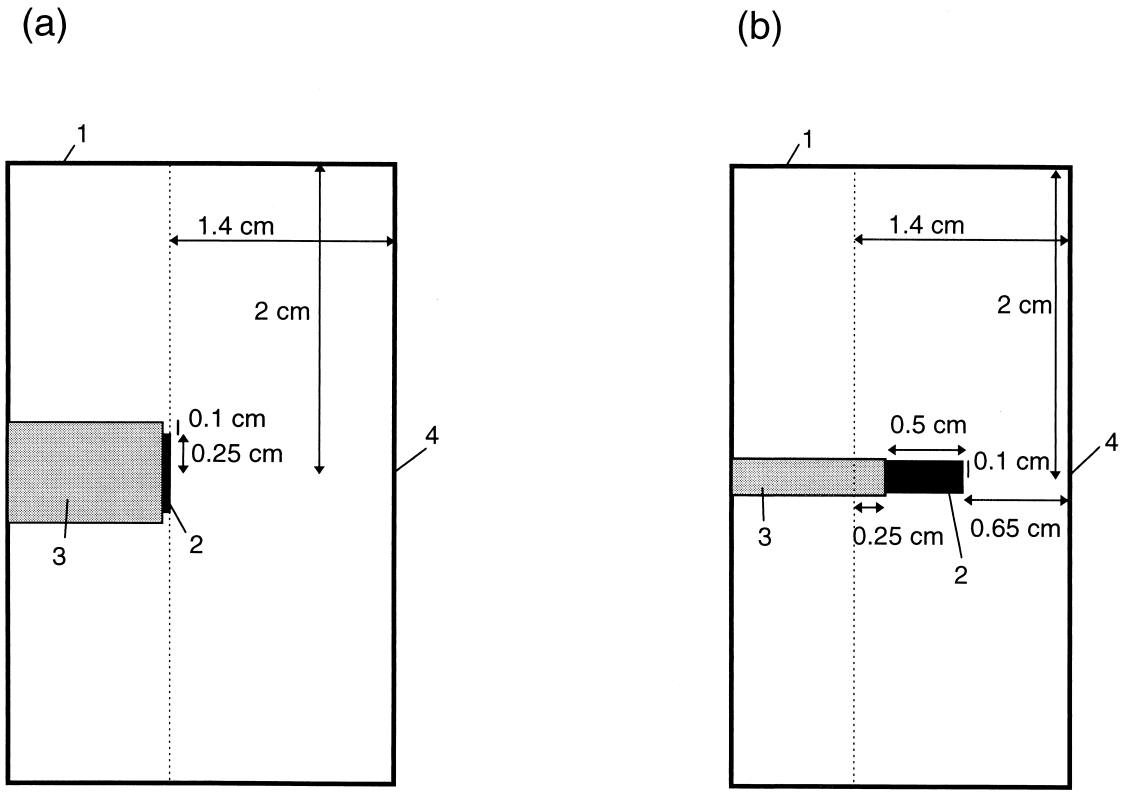

Figure 1. Schematic overview of the glow discharge cells with (**a**) flat, and (**b**) pin-type cathode. 1: cell house at anode potential; 2: cathode (made of copper); 3: direct insertion probe (made of teflon); 4: position of exit slit to the mass spectrometer. The vertical dashed lines represent the "pseudo-walls" of the cell; only the right part of the cell is modeled.

the argon and copper ions in the nearly field-free region of the discharge (negative glow), argon metastable atoms, and copper atoms]. Moreover, the Poisson equation is used to obtain a self-consistent electric field distribution from the calculated densities of charged plasma species. All these models are coupled due to the interaction processes among the different species and they are solved iteratively until final convergence is reached to obtain an overall picture of the glow discharge. More details about these models can be found in refs 3–5, 12, 14, and 17–21.

In the present work, the models are applied to glow discharge cells with either flat or pin-type cathodes (simply called "flat cell" and "pin cell"). These cells are shown schematically in Figure 1. Both are cylindrically symmetrical, and can therefore be represented by a two-dimensional cross section of the cylinder. In order to compare the flat and pin cell, we have chosen flat and pin cathodes of comparable dimensions (i.e., 5 mm diameter and 5 mm length, respectively). These are the typical dimensions used in a six-way cross glow discharge cell [10, 12, 13]. In the calculations, both cells are assumed to be in a closed configuration, but the position where the exit slit to the mass spectrometer would be in a glow discharge mass spectrometer, is indicated on the figures. The vertical dashed lines in the figures represent the "pseudo-walls" of the cell; only the right part of the cell is modeled. These pseudo-walls are included so that both cells have the same length which makes direct comparison possible. Moreover, their inclusion is justified, because it was experimentally observed that the glow discharge plasma is only visible to the right of the dashed lines.

Results and Discussion

The results for both cell geometries will be shown for the typical discharge conditions of 1000 V and about 2 mA. In the models, the electrical current is calculated self-consistently when voltage, pressure, and gas temperature are given. A gas temperature of 450 K was assumed in both cells. This parameter cannot easily be measured in a glow discharge. Often, room temperature is assumed, but in the literature, gas temperatures of 900–1400 K are reported in a Grimm-type glow discharge [22]. The latter operates, however, at much higher currents (i.e., 40–80 mA) than the present value of about 2 mA, so that higher gas temperatures are indeed expected than in our case. Sometimes the glow discharge cell is cooled, and can further complicate the situation (i.e., low temperatures at the walls, but maybe higher temperatures in the plasma). Moreover, we found that small variations in the gas temperature had a significant effect on the calculations (e.g., 30% varia-

tion in gas temperature yielded a factor of 2 variation in electrical current). The value of 450 K was therefore chosen, because it appears to be a realistic value and it leads to reasonable current values.

At 1000 V discharge voltage and 450 K gas temperature, a current of about 2.2 mA was obtained for a gas pressure of 1 torr in the case of the flat cell, and for 0.7 torr in the pin cell. Hence, in a pin cell a lower pressure suffices to yield the same current-voltage values as for a flat cell. Or, in other words, the same voltage and pressure values result in a higher current in a pin cell compared to a flat cell. Indeed, for a pin cell at 1 torr and 1000 V, a current of 8.5 mA was calculated. It can be seen that the effect is not linear: a small variation in pressure (e.g., 0.7–1 torr: 35% difference) gives rise to a larger variation in current (i.e., 2.2–8.5 mA: factor of 4 difference). Indeed, an increase in pressure results in a higher gas atom number density, and hence in more collisions. More ionization collisions yield the creation of more electrons and ions that can again produce more ionization collisions giving rise to more production of electrons and ions, etc. (i.e., snowball effect). Since electrons and ions are the current carriers in the glow discharge, it can be easily understood that an increase in pressure leads therefore to a higher current.

The reason for the lower pressure at constant current and voltage, or the higher current at constant voltage and pressure, in the case of the pin cathode, is that the latter has a considerably larger area exposed to the discharge than the flat cathode, although the dimensions of both flat and pin cathode are comparable (see before). Indeed, $2\pi rL + \pi r^2 = 0.345$ cm^2 for the pin cathode, and $\pi r^2 = 0.196$ cm^2 for the flat cathode; the sides of the flat cathode are not taken into account because of their small area and because the glow discharge plasma is primarily situated in front of the flat cathode. In general it appears from the calculations that the discharge conditions (pressure, voltage, current) do not specifically depend on the shape of the cathode, but strongly depend on the cathode area exposed to the discharge.

Because current and voltage are the two discharge parameters that are more readily available than the pressure (i.e., they can be more easily measured, whereas the pressure often cannot be measured in the glow discharge cells; sometimes only an indication is given, based on the gas flow at the gas inlet port), a comparison will be made between flat and pin cells at the same voltage and current (1000 V and 2.2 mA) and a different pressure (1 torr and 0.7 torr, respectively), but the results for the pin cell at 1 torr will also be mentioned.

Figure 2 illustrates the calculated potential distribution throughout the cell for the flat (a) and pin (b) cell. In the flat cell (Figure 2a), the cathode is represented by the black line at z = 0 and r = 0; the pin cathode in Figure 2b is also given by the black rectangle, and the shaded rectangle stands for the insertion probe. The potential is at −1000 V at the cathode. It increases rapidly and goes through zero at a few mm from the cathode; it is slightly positive in the rest of the plasma and returns to zero at the anode walls. The position where the potential crosses the zero line is defined here as the interface between cathode dark space (CDS; where the potential varies strongly, yielding a high electric field) and negative glow (NG; where the potential is more or less constant, resulting in a nearly field-free region). In the case of the flat cell, this interface is at about 1.5 mm from the cathode, whereas in the pin cell, the interface is located at about 2.6 mm from the cathode (both at the side and at the top). This slightly longer CDS length in the pin cell is entirely due to the lower pressure, because the CDS length increases significantly with decreasing pressure [5, 14]. Indeed, at 1 torr, the CDS-NG interface for the pin cell was also located at 1.5 mm from the cathode. Hence, it appears that at a constant pressure, the cell shape has no influence on the length of the CDS. The value of the potential in the rest of the plasma (i.e., in the NG; called the plasma potential) was also comparable for both cell geometries.

In Figure 3, the argon ion density profiles, for both the flat (a) and pin (b) cells are presented. The argon ion density is low and more or less constant in the CDS and reaches its maximum at about 5 mm from the cathode, in both cells. In the flat cell, the maximum is at the cell axis, whereas in the pin cell, the maximum is confined to a ring around the pin at about 6 mm off-axis. Comparing the absolute values of the two maxima (i.e., about 2.1×10^{12} cm^{-3} for the flat cell, and about 2.9×10^{11} cm^{-3} for the pin cell), it can be seen that the argon ion density in the pin cell is almost a factor of 10 lower than the corresponding density in the flat cell, although the fluxes of argon ions in both types of cells are comparable (i.e., they determine the electrical current of 2.2 mA). The reason for this is twofold: (i) in the pin cell there are relatively more "walls" (i.e., the pin itself) at which the argon ions can become neutralized, resulting in a lower density in the plasma; and (ii) moreover, the pin cell is operated at a lower pressure, yielding higher diffusion coefficients and hence a lower argon ion density. Indeed, the pin cell operating at 1 torr yielded an argon ion density at the maximum of 2.5×10^{12} cm^{-3} that is even higher than for the flat cell (see above), due to the higher electrical current (i.e., 8.5 mA versus 2.2 mA).

The slow electron density is characterized by nearly the same profile as the argon ion density: it is more or less equal to the argon ion density profile in the NG, but it is zero in the CDS (there are no slow electrons in the CDS, because they would be accelerated immediately by the strong electric field, and hence they belong to the fast electron group). This results in nearly charge neutrality in the NG and a positive space charge in the CDS that gives rise to the potential distributions shown in Figure 2. The fast electron density profile reaches its maximum in the beginning of the NG, i.e., for the flat cell at about 2 mm from the cathode, and for the pin cell

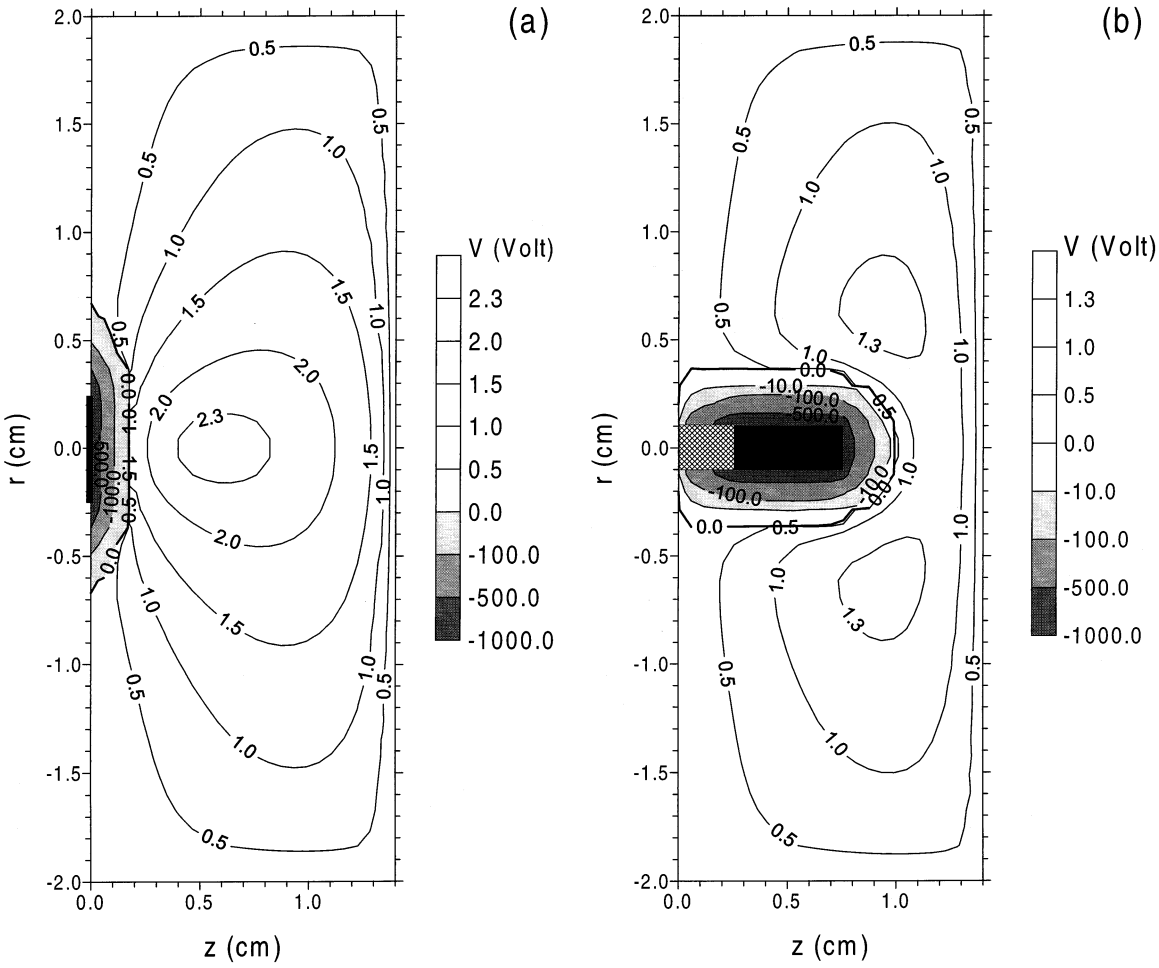

Figure 2. Calculated potential distribution throughout the flat (**a**) and pin (**b**) glow discharge cell (copper cathode in argon, 1000 V, 2.2 mA, 1 and 0.7 torr, respectively).

on a ring around the pin, located at about 3 mm from the cathode pin (similar to the argon ion density).

The density profiles of the argon metastable atoms in the flat and pin cells are shown in Figure 4 (a and b, respectively). The density reaches a maximum close to the cathode (at about 1 mm on the cell axis for the flat cell and in a ring close to the pin side for the pin cell). This distinct maximum is because of the relative importance of different production and loss processes [4, 20]. The most important production processes are electron impact excitation (especially in the beginning of the NG) and fast argon ion and atom impact excitation (only important in the CDS, close to the cathode, where the ions and atoms can reach high energies). The loss of the metastable atoms appears to occur primarily by electron collisional transfer to the nearby resonant levels (especially in the NG where the electron density is at its maximum; see above) and by diffusion and subsequent deexcitation at the walls. Penning ionization of sputtered atoms and metastable atom–metastable atom collisions also play a small but non-negligible role. The pronounced peak close to the cathode is because of the high production of metastables by fast argon ion and atom impact excitation, and no loss process is really able to compensate for this high production. Further away from the cathode, in the NG, the density of metastable atoms decreases, because the production by electron impact excitation is efficiently compensated by loss processes (primarily electron collisional transfer to the nearby levels; see above). More information about the relative contributions of the various production and loss processes, and about their effect on the metastable atom density can be found in refs 4, 13, and 20.

The maximum density in the pin cell (i.e., $\sim 9 \times 10^{11}$ cm^{-3}) is a factor of 2 lower than in the flat cell (i.e., $\sim 2 \times 10^{12}$ cm^{-3}); however, the density further in the discharge, and especially at the position of the exit slit to the mass spectrometer if the glow discharge is used for mass spectrometry (see Figure 1), is slightly higher for the pin cell, compared to the flat cell, as can be seen in Figures 4a and 4b.

In Figure 5, the sputtered copper atom density profiles are illustrated for the flat (a) and the pin cell (b). The copper atom densities, both in the flat and the pin cell reach a maximum at 1 mm from the cathode and decrease towards the cell walls. In the pin cell the

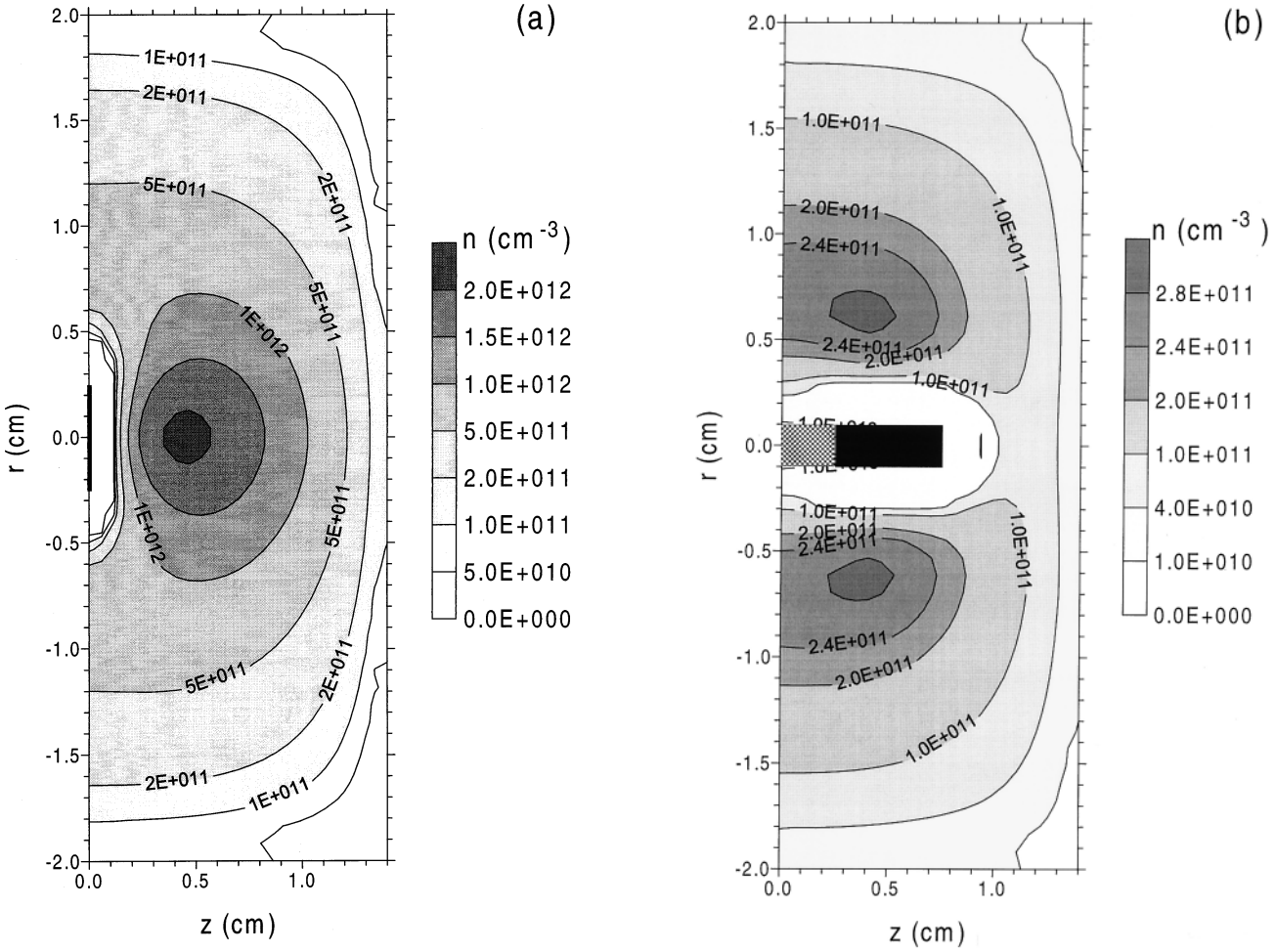

Figure 3. Calculated density profile of the argon ions throughout the flat (**a**) and pin (**b**) glow discharge cell (copper cathode in argon, 1000 V, 2.2 mA, 1 and 0.7 torr, respectively).

maximum is, however, a factor of 3–4 lower (i.e., 6.8×10^{12} cm^{-3} compared to 2.2×10^{13} cm^{-3} for the flat cell), for the same reasons as above (see discussion for the argon ion density). However, the values further in the discharge (e.g., at the exit slit to the mass spectrometer) are slightly higher in the pin cell than in the flat cell, as seen in Figure 5a and b. This is expected because in the pin cell, the exit slit is closer to the cathode that is the source of the copper atoms. The copper atom density calculated for the pin cell at 1 torr reaches a maximum of about 4.2×10^{13}, which is a factor of 2 higher than for the flat cell at 1 torr, due to the higher current.

The maximum at the sides of the pin is slightly higher than at the top of the pin, as was also the case for the other plasma species densities. It appears that the glow discharge plasma is more intense at the sides than at the top of the pin. It was calculated that about 93% of the total sputtering originated from the sides of the pin, whereas only about 7% of the sputtering took place at the top of the pin. This is in close correlation with the respective cathode areas exposed to the discharge (i.e., the side and top of the pin contribute about 91% and 9% to the total surface area exposed to the discharge, respectively).

Sputtering on the cathode is caused by the bombardment of plasma species. It only becomes important at kinetic energies of the bombarding species of tens of eV and higher. In practice, only ions (both argon and copper ions) and fast argon atoms play a role in sputtering. Indeed, the ions are directed towards the cathode by the strong electric field in front of it and they gain high kinetic energies from this electric field; the fast argon atoms are created from the argon ions on their way towards the cathode by symmetric charge transfer and elastic collisions. They hereby obtain energies comparable to the argon ion energy, and they continue more or less in the same way as the ions so that they will also bombard the cathode with appropriate energies for sputtering. Argon metastable atoms, thermal argon atoms, and copper atoms are not able to produce sputtering, because they have nearly thermal energies in the glow discharge. It was calculated that the contributions of argon ions, fast argon atoms, and copper ions to the total amount of sputtering are about

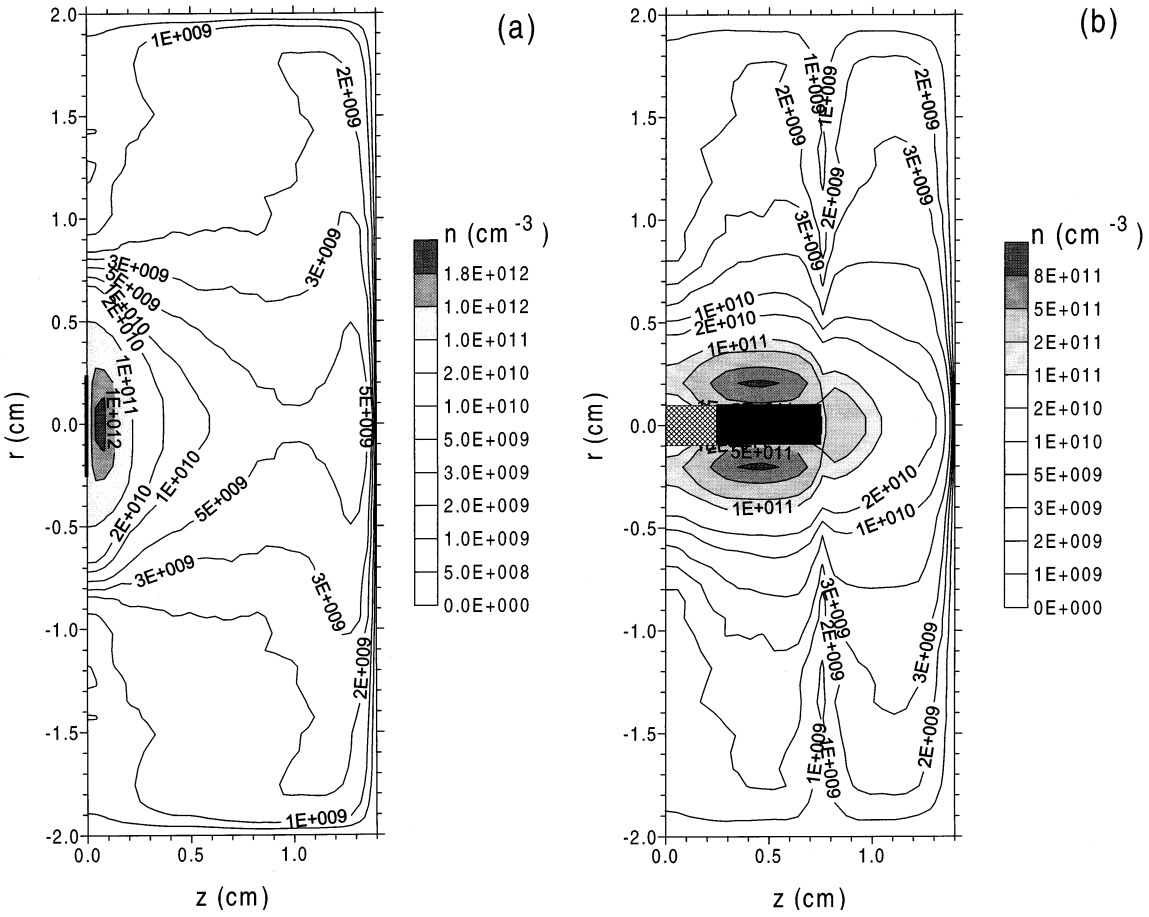

Figure 4. Calculated density profile of the argon metastable atoms throughout the flat (**a**) and pin (**b**) glow discharge cell (copper cathode in argon, 1000 V, 2.2 mA, 1 and 0.7 torr, respectively).

28%, 70%, and 2%, respectively, for both the flat and the pin cell.

The copper ion density profiles are given in Figure 6, for both the flat (a) and pin cell (b). The qualitative appearance of these profiles is similar to the argon ion density profiles, i.e., low and rather constant in the CDS and at their maximum at about 5 mm from the cathode. The absolute values are, however, almost two orders of magnitude lower. The maximum in the pin cell (i.e., $\sim 3.4 \times 10^9$ cm^{-3}) is a factor of 10 lower than the corresponding value in the flat cell (i.e., $\sim 4.4 \times 10^{10}$ cm^{-3}), the reasons being (i) the lower pressure in the pin cell, resulting in higher diffusion coefficients and hence lower densities, (ii) the greater role of the discharge walls (i.e., the pin itself), yielding more neutralization at the walls and hence lower densities, (iii) the lower copper atom density, and (iv) the lower argon ion (and metastable argon atom) densities that are necessary for the ionization of copper (i.e., by asymmetric charge transfer and Penning ionization, respectively). The ionization degree of copper was indeed calculated to be clearly lower in the pin cell than in the flat cell (i.e., $\sim$0.2% versus $\sim$1.3%), which is especially attributed to the lower argon ion density and hence decreasing importance of asymmetric charge transfer. Indeed, the relative contributions of Penning ionization, asymmetric charge transfer, and electron impact ionization to the total ionization of the copper atoms amount to about 16%, 81.5%, and 2.5% for the flat cell, and to about 38.5%, 59%, and 2.5% for the pin cell. Hence, asymmetric charge transfer ionization seems indeed to be less important for the pin cell, whereas Penning ionization becomes relatively more important (as could also be expected from the somewhat higher metastable density close to the end of the cell). At a pressure of 1 torr, the copper ion density at the maximum of its profile was calculated to be 2.6×10^{11} cm^{-3}, the ionization degree was 2.4%, and the relative contributions of Penning ionization, asymmetric charge transfer, and electron impact ionization to the total ionization of copper amounted to about 7%, 91%, and 2%, respectively. Hence, at the same pressure, the ionization of copper is somewhat more efficient than in the flat cell, particularly due to the higher argon ion density and the more important role of asymmetric charge transfer. The more efficient ionization, combined with the higher copper atom density, results in a considerably higher copper ion density in the pin cell compared to the flat cell at the same pressure (but lower current).

In ref 23 it was suggested that the relative contribu-

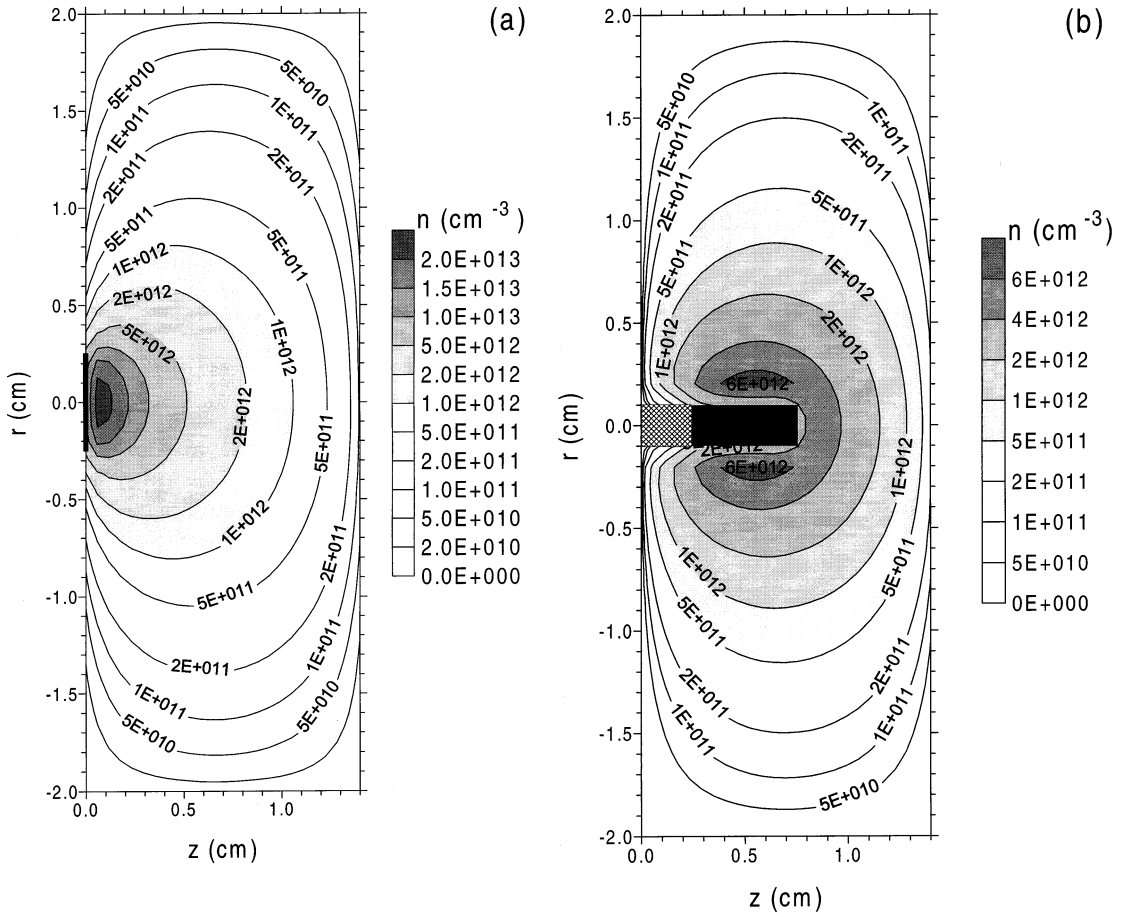

Figure 5. Calculated density profile of the sputtered copper atoms throughout the flat (**a**) and pin (**b**) glow discharge cell (copper cathode in argon, 1000 V, 2.2 mA, 1 and 0.7 torr, respectively).

tions of Penning ionization and asymmetric charge transfer affect the relative sensitivity factors (RSF) in glow discharge mass spectrometry. Therefore, since both these processes are of different relative importance in the flat and the pin cell, it can be expected that the RSF values may be different for these two cell geometries. This was also found experimentally. Indeed, in ref 9 it was demonstrated that the RSFs in pin and flat cells are different for nonconducting samples. In general, the RSFs for flat samples were found to be more uniform than for pin samples. The exact experimental behavior cannot yet be predicted in detail by our model (also because the experimental conditions and cell geometries are different from the ones used in our model), but our expectations that RSF will be different for flat and pin cells are at least qualitatively backed up by the experiment.

When the glow discharge is used as an ion source for mass spectrometry, special interest goes to the values of the ion currents at the exit slit towards the mass spectrometer. It was calculated that the argon ion fluxes at the exit slit were about 5.2×10^{15} cm^{-2} s^{-1} for the flat cell (at 1000 V, 2.2 mA, and 1 torr) and about 7.7×10^{14} cm^{-2} s^{-1} the pin cell (at 1000 V, 2.2 mA, and 0.7 torr), respectively. Assuming an exit slit area of about 0.001 cm^2 (e.g., 1 mm long and 0.1 mm wide), this results in argon ion currents leaving the cell of about 8.3×10^{-7} A and 1.2×10^{-7} A for the flat and pin cell, respectively (1 A is about 6.24×10^{18} ions per s). The corresponding copper ion fluxes at the exit slit of the cell were calculated to be about 1.1×10^{14} cm^{-2} s^{-1} and 9.1×10^{12} cm^{-2} s^{-1}, for the flat and pin cell, respectively, at the same discharge conditions as mentioned above. This results in copper ion currents leaving the cell of about 1.8×10^{-8} A and 1.5×10^{-9} A, for the flat and pin cell, respectively. The ratios of copper ion to argon ion currents leaving the glow discharge cell amount then to about 2.2% and 1.3%, for the flat and pin cell. Hence, it seems that for the present conditions, the flat cell yields higher currents of argon ions, copper ions, and higher ratios of copper to argon ion currents leaving the glow discharge cell and entering the mass spectrometer. This also means better analytical sensitivity. However, it should again be stressed that the pressure in the pin cell is lower than in the flat cell. At the same pressure of 1 torr, the pin cell yields values of the argon ion current, copper ion current, and ratio of copper to argon ion current at the exit slit, of about 8.6×10^{15} cm^{-2} s^{-1}, 4.5×10^{14} cm^{-2} s^{-1}, and 5.2%, respectively, which is

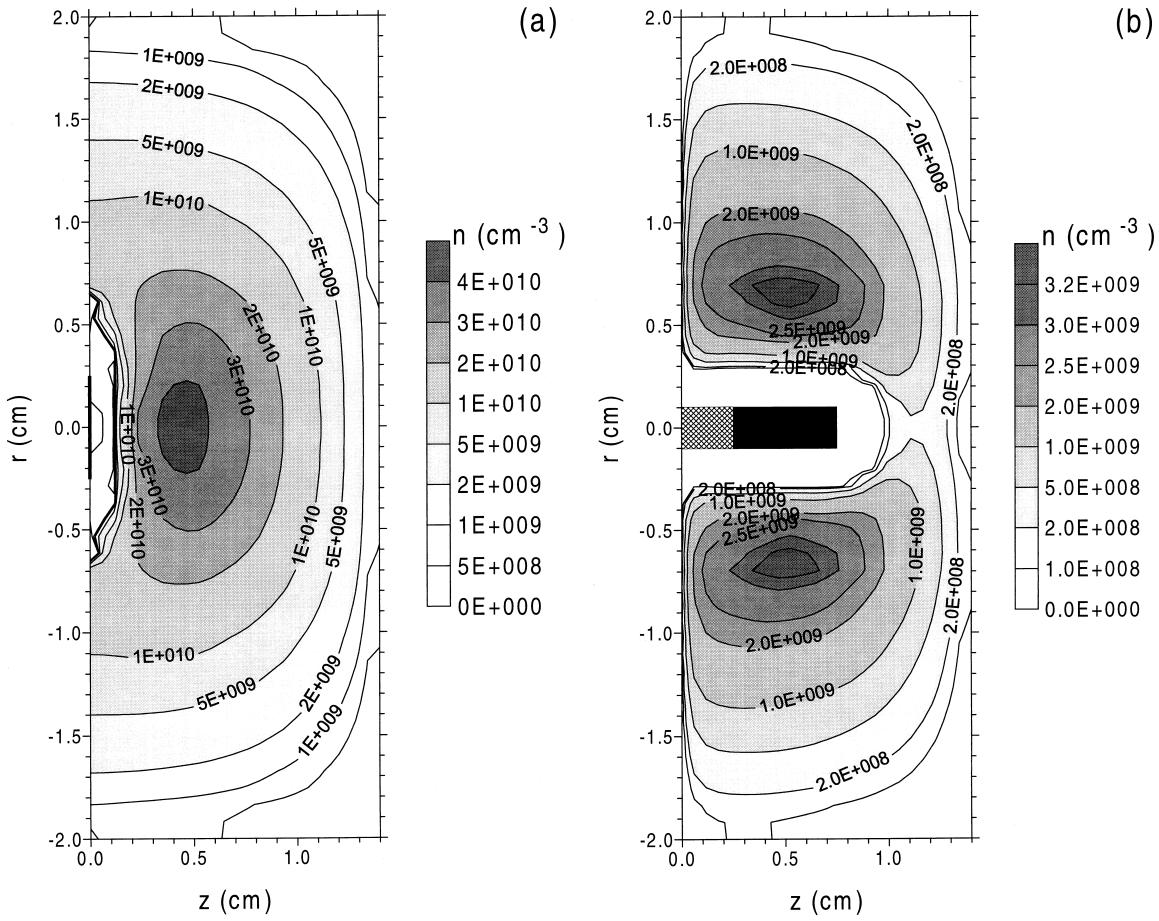

Figure 6. Calculated density profile of the copper ions throughout the flat (**a**) and pin (**b**) glow discharge cell (copper cathode in argon, 1000 V, 2.2 mA, 1 and 0.7 torr, respectively).

igher than for the flat cell at the same pressure, resulting therefore in a better analytical sensitivity.

Finally, we studied the influence of the sampling distance (i.e., distance between cathode pin and anode exit slit) on the calculated quantities, and the results are summarized in Table 1. A similar study was carried out already for the flat cell in [7], and will therefore not be repeated here. It appears that when increasing the distance from 0.25 cm to 0.85 cm, the electrical current also increases slightly. The reason is that the discharge cell becomes somewhat larger (i.e., the length of the cell increases from 1.0 cm to 1.6 cm; see Figure 1b), so that more ionization collisions can take place, yielding a higher production of current carriers (electrons and ions), and hence a higher electrical current. Because the current rises slightly with increasing distance, the densities of the plasma species rise accordingly, as can be seen from Table 1. The increase is largest for the copper ions, because there is a double effect: (i) the copper atom density, and (ii) the amount of ionization of copper (determined by the argon metastable atom, argon ion, and electron densities) both increase with larger dis-

Table 1. Influence of the sampling distance (i.e., distance between cathode pin and exit slit) on the calculated quantities (pin cell, at 1000 V and 0.7 torr)

Sampling distance	0.25 cm	0.45 cm	0.65 cm	0.85 cm
Electrical current (mA)	1.6	2.0	2.2	2.4
Ar^+, slow electron density (cm^{-3})	1.6×10^{11}	2.5×10^{11}	2.9×10^{11}	3.4×10^{11}
Fast electron density (cm^{-3})	1.4×10^{7}	2.0×10^{7}	2.2×10^{7}	2.3×10^{7}
Ar^*_{met} density (cm^{-3})	7.9×10^{11}	9.5×10^{11}	9.6×10^{11}	1.0×10^{12}
Cu^0 density (cm^{-3})	4.2×10^{12}	6.5×10^{12}	6.8×10^{12}	8.0×10^{12}
Cu^+ density (cm^{-3})	1.0×10^{9}	2.5×10^{9}	3.4×10^{9}	6.8×10^{9}
Ionization degree of Cu (%)	0.06	0.12	0.17	0.24
Ar^+ flux at exit slit ($cm^{-2}\ s^{-1}$)	0.0	2.3×10^{14}	7.7×10^{14}	1.5×10^{15}
Cu^+ flux at exit slit ($cm^{-2}\ s^{-1}$)	0.0	2.3×10^{12}	9.1×10^{12}	3.1×10^{13}

tances. The latter effect is also reflected in the ionization degree of copper, presented in Table 1. Also the argon and copper ion fluxes at the exit slit towards the mass spectrometer rise clearly with increasing distance. The ion fluxes for the shortest sampling distance were calculated to be virtually zero, because the cathode pin is so close to the exit slit that the ions at the exit slit are still attracted towards the cathode by the strong electric field in front of it. In reality, there will be a net ion flux leaving the cell, because of the extraction field or pressure gradient that draws ions outside the cell into the mass spectrometer.

The increase of ion fluxes with rising sampling distance would indicate that at larger pin-exit slit distances the ion currents in the mass spectrum increase, and hence the analytical sensitivities become better. In [10], the influence of the pin-exit slit distance on the analytical results was investigated for nonconductors, and it was found that in the direct current (dc) case, the signal intensity in the mass spectrum increased with longer sampling distances. This is in qualitative agreement with our findings. However, this agreement should be considered with caution, because we investigated sampling distances of 0.25–0.85 cm, while those studied in ref 10 varied from 0.5–1.1 cm, and also the discharge conditions were not exactly the same. It is expected that the analytical sensitivity as a function of sampling distance probably goes through a maximum, depending on the discharge conditions. Indeed, at short distances, the plasma is somewhat restricted in place, and increasing the distance allows the plasma to spread out more throughout the cell and become more intense. However, at long distances the plasma will not extend any further [7], and increasing the distance causes the cathode pin [source of sputtered (analyte) species] to be further away from the exit slit to the mass spectrometer.

Conclusion

Three-dimensional models for an analytical direct current glow discharge have been applied to cell geometries with flat and pin-type cathodes. It was found that for the pin cell, the plasma is most intense around the sides of the pin and is weaker at the top of the pin. The qualitative trends in most of the calculated results were comparable, but some variations in quantitative results have been found, e.g., in the current-voltage-pressure relations, the densities of the plasma species, and the ion currents leaving the cell and entering the mass spectrometer (this determines the analytical sensitivity). Also the relative contributions of Penning ionization and asymmetric charge transfer to the ionization of the sputtered copper atoms were somewhat different for the pin and the flat cell. Since the relative contributions of both these ionization processes must affect the relative sensitivity factors (RSF) in glow discharge mass spectrometry, it can be expected that the RSF values will not necessarily be the same for pin and flat cells. This was also experimentally observed in the literature.

In the case of the pin cell, the influence of sampling distance on the calculated results was investigated; it was found that maximum ion currents (and hence analytical sensitivity) were reached for the longer pin to exit slit distances. This is in agreement with experimental observations in the literature.

Finally, in the present article the authors wanted to show that this type of modeling may be useful in expediting experimental design.

Acknowledgments

A. B. is indebted to the Fund for Scientific Research (FWO)—Flanders. The authors also acknowledge financial support from the Federal Services for Scientific, Technical and Cultural Affairs (DWTC/SSTC) of the Prime Minister's Office through IUAP-III (Conv. 49) and IUAP-IV (Conv. P4/10). Finally, the authors wish to express their gratitude to Dr. W. Goedheer for the many helpful discussions.

References

1. Marcus, R. K., *Glow Discharge Spectroscopies*; Plenum Press: New York, 1993.
2. Chapman, B., *Glow Discharge Processes*; Wiley: New York, 1980.
3. Bogaerts, A.; Gijbels, R.; Goedheer, W. J., *Anal. Chem.* **1996,** *68*, 2296–2303.
4. Bogaerts, A.; Gijbels, R., *Anal. Chem.* **1996,** *68*, 2676–2685.
5. Bogaerts, A., *Ph.D. Dissertation*, University of Antwerp, 1996.
6. Bogaerts, A.; Gijbels, R., *Spectrochim. Acta B* **1997,** *52*, 553–566.
7. Bogaerts, A.; Gijbels, R., *J. Anal. At. Spectrom.*, in press.
8. Teng, J.; Barshick, C. M.; Duckworth, D. C.; Morton, S. J.; Smith, D. H.; King, F. L., *Appl. Spectrosc.* **1995,** *49*, 1361–1366.
9. De Gendt, S.; Schelles, W.; Van Grieken, R.; Müller, V., *J. Anal. At. Spectrom.* **1995,** *10*, 681–687.
10. De Gendt, S.; Van Grieken, R.; Hang, W.; Harrison, W. W., *J. Anal. At. Spectrom.* **1995,** *10*, 689–695.
11. Hang, W.; Walden, W. O.; Harrison, W. W., *Anal. Chem.* **1996,** *68*, 1148–1152.
12. Bogaerts, A.; Wagner, E.; Smith, B. W.; Winefordner, J. D.; Pollmann, D.; Harrison, W. W.; Gijbels, R., *Spectrochim. Acta B* **1997,** *52*, 205–218.
13. Bogaerts, A.; Guenard, R. D.; Smith, B. W.; Winefordner, J. D.; Harrison, W. W.; Gijbels, R., *Spectrochim. Acta B* **1997,** *52*, 219–229.
14. Bogaerts, A.; Gijbels, R., *J. Appl. Phys.* **1995,** *78*, 6427–6431.
15. van Straaten, M.; Bogaerts, A.; Gijbels, R., *Spectrochim. Acta B* **1995,** *50*, 583–605.
16. Bogaerts, A.; Gijbels, R., *Spectrochim. Acta B* **1997,** *52*, 765–778.
17. Bogaerts, A.; van Straaten, M.; Gijbels, R., *Spectrochim. Acta B* **1995,** *50*, 179–196.
18. Bogaerts, A.; van Straaten, M.; Gijbels, R., *J. Appl. Phys.* **1995,** *77*, 1868–1874.
19. Bogaerts, A.; Gijbels, R.; Goedheer, W. J., *J. Appl. Phys.* **1995,** *78*, 2233–2241.
20. Bogaerts, A.; Gijbels, R., *Phys. Rev. A* **1995,** *52*, 3743–3751.
21. Bogaerts, A.; Gijbels, R., *J. Appl. Phys.* **1996,** *79*, 1279–1286.
22. Ferreira, N. P.; Human, H. G. C.; Butler, L. R. P., *Spectrochim. Acta B* **1980,** *35*, 287–295.
23. Bogaerts, A.; Gijbels, R., *J. Anal. At. Spectrom.* **1996,** *11*, 841–847.